Center for Turbulence Research
Proceedings of the Summer Program 1992

A transport equation for eddy viscosity

By P. A. Durbin[1] AND Z. Yang[2]

A transport equation for eddy viscosity is proposed for wall bounded turbulent flows. The proposed model reduces to a quasi-homogeneous form far from surfaces. Near to a surface, the nonhomogeneous effect of the wall is modeled by an elliptic relaxation model. All the model terms are expressed in local variables and are coordinate independent; the model is intended to be used in complex flows. Turbulent channel flow and turbulent boundary layer flows with/without pressure gradient are calculated using the present model. Comparisons between model calculations and direct numerical simulation or experimental data show good agreement.

1. Introduction

Algebraic turbulence models (Baldwin-Lomax 1978, Cebeci-Smith 1974) have been used extensively in calculations of aerodynamic flows. These algebraic models are easy to implement numerically and give accurate predictions for simple flows, such as that over an airfoil with an attached boundary layer; however, they are inadequate when used for more complex flows, such as that over an airfoil with separation. In addition, these models contain nonlocal parameters in their formulations. The interpretation of these parameters becomes ambiguous in complex geometries. Higher order turbulence models have been proposed to overcome deficiencies of these algebraic models, the most popular among these being the $k-\epsilon$ model. The empirical constants in the $k-\epsilon$ model have been optimized in a variety of simple shear flows, giving what is commonly referred to as the Standard $k-\epsilon$ model (Launder and Spalding 1974, Rodi 1980).

The Standard $k-\epsilon$ model was devised for turbulence far away from boundaries. For near wall turbulence, the model either has been used in conjunction with wall functions or has been modified by damping functions and other near wall terms to give the so called near wall version of the $k-\epsilon$ model. This fixed up model can be integrated down to the wall.

In the wall function approach, one assumes the existence of a universal wall layer, which is not valid in many complex flows. In the damping function approach, the results depend on the damping functions used—a wide variety of which have been proposed. These damping functions themselves must be assumed to be of a universal form.

It is also found that for near wall flows the $k-\epsilon$ model is numerically stiff: it requires many grid points near the wall to get a grid independent solution. This

1 Center for Turbulence Research
2 ICOMP/NASA Lewis Research Center

numerical stiffness makes the model rather unappealing for aerodynamic computations. The numerical stiffness of the $k-\epsilon$ model is partly due to the rapid variation of ϵ (and to a less extend k) near the wall.

The eddy viscosity, ν_t, varies much more gradually near the wall. This observation suggests that an equation for the eddy viscosity might be less stiff; this was one motivation for the work of Baldwin and Barth (1990) and Spalart and Allmaras (1992). In these papers, a transport equation for eddy viscosity of the type originally proposed by Nee and Kovasznay (1968) was formulated and solved in conjunction with the mean field equations. Wall effects were introduced in these models by damping functions, in which the distance to the wall y enters as an parameter. This wall distance y is not a local property; its definition may be ambiguous for flows in complex geometry—corner flow for example. Also, the damping functions are assumed to be universal, which does not seem valid in flows with strong adverse pressure gradients and separation.

Modeling of near wall turbulence is very important for engineering calculation because the near wall portion of the boundary layer contributes substantially to the total momentum and heat transfer. In the near wall region, the turbulence is strongly inhomogeneous and strongly anisotropic. Recently, Durbin (1991) introduced the method of elliptic relaxation to model the blocking effect of the wall on the turbulence. In this method, the behavior of the near wall turbulence is given by the solution of an (elliptic) differential equation rather than by prescribed algebraic expressions. Geometric information enters through the boundary conditions enforced at the wall. Thus, it is hoped that this formulation can handle flows in complex geometry. This approach also has the appeal that it is coordinate independent.

In the present work, we propose a new transport model for the eddy viscosity. Far away from the wall, the model is based on the quasi-homogeneous approximation; near the surface, the wall effect is introduced via an elliptic relaxation equation. The structure of the paper is as follows: the proposed model is presented in section 2; in section 3, we show calculations of turbulent channel flow and turbulent boundary layer flows with and without pressure gradient; section 4 concludes the paper.

2. The proposed model

2.1 The eddy viscosity

In the framework of the eddy viscosity model, the unknown Reynolds stress $-\overline{u_i u_j}$ in the mean momentum equation is assumed to be related to the mean velocity field by

$$-\overline{u_i u_j} = 2\nu_t S_{ij} - \frac{2}{3}k\delta_{ij} \tag{1}$$

where S_{ij} is the strain rate of the mean field and ν_t is the eddy viscosity. The last term in (1), containing the turbulent kinetic energy k, can be absorbed into the mean pressure. Thus, only the eddy viscosity needs to be modeled.

We propose that the general form of a transport equation for the eddy viscosity be

$$\frac{D}{Dt}\nu_t = \nabla\cdot\left[\left(\nu + \frac{\nu_t}{\sigma}\right)\nabla\nu_t\right] + \Phi \tag{2}$$

where the turbulent self transport is assumed to be analogous to the laminar diffusion and Φ is a source term representing the *combined effect* of production and dissipation of ν_t. Our objective is to propose a model for Φ which is valid for both near wall and free shear layers. The justification for using a scalar eddy viscosity, as in (1), is that our attention is on thin shear layers, in which transport is predominantly transverse to the shear.

2.2 Model for flow away from the wall

Far from the solid surface, the inhomogeneity of a turbulence field is relatively weak. The model for Φ could then be found by expanding about the homogeneous state. This quasi-homogeneous case is considered first.

For homogeneous shear flow, if ν_t is much larger than ν, the only variables that can enter the problem are the eddy viscosity ν_t and the shear rate S. (The shear rate S will be defined here via the rate of strain tensor of the mean field: $S = 2(S_{ij}S_{ji})^{1/2}$.) From dimensional reasoning, we have

$$\Phi = \Phi(S, \nu_t) = c_1 S \nu_t \tag{3}$$

where c_1 is a model constant. Experimental results for homogeneous shear flow give $c_1 \approx 0.12$.

In general, the flow is not homogeneous. Flow inhomogeneity can be represented by $|\nabla \nu_t|$ and by $|\nabla S|$, which are measures of the inhomogeneity of the turbulence field and of the mean field, respectively. If the inhomogeneity is weak, expansion about the homogeneous state suggests the form

$$\Phi = c_1 S \nu_t - c_2 |\nabla \nu_t|^2 - c_3 \frac{\nu_t^2}{L_\nu^2}, \tag{4}$$

where the length scale L_ν is given by

$$L_\nu^{-2} = \left(\frac{|\nabla S|}{S} \right)^2 . \tag{5}$$

Other terms, such as $|\nabla \nu_t| \nu_t / L_\nu$ might be considered; (4) is analogous to the forms selected by Baldwin and Barth (1990) and Spalart and Almaras (1992). The model (4) allows inhomogeneities in both the turbulent field and the mean field to contribute to 'dissipation' of the eddy viscosity.

2.3 Model for near wall turbulence

Eq (4) is based on an expansion near the homogeneous state. The expansion is valid only for weak inhomogeneity. In the near wall region the flow changes very rapidly to adjust to the boundary condition at the wall; thus, the flow field is strongly inhomogeneous, and the expansion about the homogeneous state is not expected to be valid. (Direct application of equation (2) with Φ given by equation (4) to turbulent channel flow at $Re_\tau = 395$ leads to a value of the skin friction coefficient too high by about 30%.) In the present work, this strong inhomogeneity

is modeled by the elliptic relaxation model first proposed by Durbin (1991) for Reynolds stress closures.

In the Reynolds stress transport equation, the velocity-pressure gradient correlation term is a good candidate for this type of relaxation because pressure is elliptic in nature. In the transport equation for the eddy viscosity, the pressure term does not appear explicitly; which term should be operated on by elliptic relaxation is questionable. An examination of the transport equation for $-\overline{uv}/S$ in simple shear flows reveals that there are two origins for the elliptic relaxation: the velocity-pressure gradient correlation and the representation of $\overline{v^2}$ in terms of $\overline{uv}$. The combination of these two effects suggests, in the case of the eddy viscosity transport model, that we write $c_1 = c_{11} - c_{12}$ and introduce the elliptic relaxation such that the transport equation appears as

$$\frac{D}{Dt}\nu_t = \nabla \cdot \left[\left(\nu + \frac{\nu_t}{\sigma}\right)\nabla\nu_t\right] + P_\nu - c_{12}S\nu_t - c_3\frac{\nu_t^2}{L_\nu^2} \tag{6}$$

where P_ν is the quantity subject to relaxation. It is governed by the elliptic equation

$$L_p^2\nabla^2 P_\nu - P_\nu = -(c_{11}S\nu_t - c_2|\nabla\nu_t|^2). \tag{7}$$

In (7), L_p is the blocking length scale and is given by

$$L_p^2 = c_p^2 \max\left(\frac{\nu_t}{S}, c_l^2\frac{\nu}{S}\right). \tag{8}$$

The first term in the 'max' function represents the turbulent length scale, which is appropriate away from the wall; the second term is chosen very close to the wall, where the appropriate length is the Kolmogorov scale. The switching from one length scale to the other is controlled by the value of c_l and the total length scale is controlled by c_p.

2.4 Modification near $S = 0$

Equations (5) and (8) give expressions for the length scales. These estimates break down when $S = 0$. $S = 0$ can occur at the edge of a boundary layer or inside a turbulent field, for example at the centerline of channel flow. A revision to the length scale formulation is needed to accommodate these cases. The singularity will be removed by the following modification:

$$L_\nu^2 = \left(\frac{S}{|\nabla S|}\right)^2 + \left(\frac{|\nabla\nu_t|}{S}\right)^2 \tag{9}$$

$$L_p^2 = \min\left[L_\nu^2, c_p^2\max\left(\frac{\nu_t}{S}, c_l^2\frac{\nu}{S}\right)\right]. \tag{10}$$

Over most of the flow field, the first term on the right hand sides of (9) and (10) is much larger than the second term. The modification only affects the region near $S = 0$.

In the course of developing and testing the model during the summer program, another modification to L_ν was inadvertently introduced: in the outermost portion of boundary layers, L_ν became constant. The algorithm was to make L_ν be independent of y when $\partial\nu_t/\partial y < 0$. ν_t decreases when y/δ_{99} is greater than ~ 0.9. In future work, this restriction will be removed; it is an effective way to avoid the difficulty of specifying L_ν in the free-stream, but its applicability is restricted to attached boundary layers.

2.5 Boundary conditions

Equations (6) and (7), together with the length scales given by (9) and (10), are the eddy viscosity model we are proposing for wall bounded turbulent flows. They form a fourth order system of equations, and, consequently, four boundary conditions are needed. These conditions are as follows: On a solid surface

$$\nu_t = \hat{n} \cdot \nabla\nu_t = 0, \tag{11}$$

where $\hat{n}$ is the surface normal; at a symmetry plane, the center line of a channel for example,

$$\nu_t' = P_\nu' = 0, \tag{12}$$

where the prime denotes the derivative normal to the symmetry plane; at the freestream edge of a boundary layer or shear layer

$$\nu_t' = P_\nu = 0. \tag{13}$$

The prime in (13) represents differentiation normal to the edge of the boundary layer. In some situations, (13) might be replaced by a condition prescribing properties of free-stream turbulence if it is present.

2.6 Model constants

There are seven empirical constants in the present model. They are σ, c_{11}, c_{12}, c_2, c_3, c_p, c_l. c_{11} and c_{12} are related by

$$c_{11} - c_{12} = c_1.$$

$c_1 \approx 0.12$ was determined by experiments on homogeneous shear flow.

Another relation among the constants is found by requiring that the model give the right behavior in the logarithmic region of a boundary layer. This imposes the constraint

$$\frac{1}{\sigma} + \frac{c_1}{\kappa^2} - c_2 = \frac{c_3}{1+\kappa^4}$$

where κ is the Von Kármán constant; we take $\kappa = 0.41$.

The constant σ in the turbulent diffusion term should be about 1 and the value of c_p, which marks the switching from the Kolmogorov length scale to the turbulent length scale, should be about 3.5. All the other constants are chosen by comparing with direct numerical simulation data for turbulent channel flow at $Re_\tau = 395$ and

with experimental data for a zero pressure gradient, flat plate boundary. The values of the constants selected in this study are

$$\sigma = 1.3,\ c_{11} = 0.4,\ c_{12} = 0.28,\ c_2 = 1.3,\ c_3 = 0.2,\ c_p = 3.5,\ c_l = 1.6\,. \qquad (14)$$

The constants listed above represent a preliminary choice: they are subject to adjustment in the course of further model development.

3. Results and discussions

Turbulent channel flows at different Reynolds numbers and turbulent boundary layers with and without pressure gradient were calculated using the present model. An implicit finite difference scheme was used to solve the momentum equation and the turbulence equations. For the present cases, the equations are parabolic and a marching scheme was used. The finite difference equations for ν_t and P_ν were solved as a coupled, block tridiagonal system. Variable grid spacing was used, with densest spacing near the wall. The total number of grid points was set to 105, which is large enough for the results to be grid independent.

Two dimensional, fully developed channel flow is attractive for model testing because it is statistically steady and nonhomogeneous in only one direction. Solutions can be found very efficiently, yet the effects of the wall on turbulent shear flow are still present. Computations were carried out for 2D fully developed turbulent channel flows at $Re_\tau = 180$ and $Re_\tau = 395$, for which DNS data are available (J. Kim, private communication). Figure 1 shows profiles of the mean velocity at these two Reynolds numbers along with DNS data. Both the dependent variable and the independent variables are represented in wall units. The predictions are in reasonable agreement with the data.

The second example calculated is the turbulent boundary layer with zero pressure gradient. The zero pressure gradient boundary layer on a flat plate has a self-similar profile (in the outer portion of the boundary layer, when scaled on outer variables). Thus, arbitrary profiles could be used as the initial conditions, and the solution should develop into its similarity form. Figure 2 shows velocity profiles scaled by the free stream velocity and the boundary layer thickness at $Re_\theta = 3195$ and $Re_\theta = 5473$, respectively. The experimental data is from Coles and Hirst (1968). It is found that indeed the velocity develops into a similarity profile, which serves as a good check for the present model. Figure 3 contains a conventional log-linear plot of the mean velocity profile. The agreement with the data is excellent except in the viscous sublayer, where the model profile is a bit low.

From an engineering point of view, the skin friction is of great interest. The skin friction coefficient as a function of Re_θ is shown in figure 4, along with experimental data (Coles and Hirst 1968). It is seen that the model gives a good prediction of C_f. The growth of the boundary layer in this range of Reynolds number is illustrated by figure 5, which shows displacement thickness as a function of Re_θ. δ_* is normalized by the boundary layer thickness at $Re_\theta = 1000$. The model gives a slight overprediction of the boundary layer growth rate.

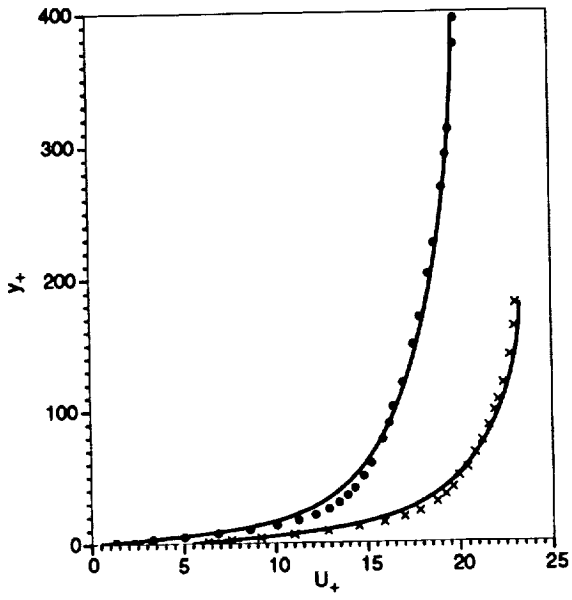

FIGURE 1. Mean velocity profiles in channel flow. •, $Re_\tau = 395$; ×, $Re_\tau = 180$. The lower Reynolds number profile is offset 5 units for clarity.

Next we calculate the development of a turbulent boundary layer in a pressure gradient. The test case chosen is the Samuel and Joubert (1974) experiment on a boundary layer developing into an increasingly adverse pressure gradient. This boundary layer is not self-similar. During the 1981-82 Stanford Conference on Complex Turbulent Flows, it was found that this flow is very difficult to predict; since then, it has become a standard test case for turbulence models.

The initial condition for the computation was set in the following manner: We assume that the turbulent boundary layer develops under zero pressure gradient up to a point, x_s say, at which the pressure gradient (which is known from the experiment) is applied. The position x_s is determined so that at the first point of the working section of wind tunnel, where the experimental data begin, the predicted values of Re_θ and C_f agree with those of the experiment.

The predicted development of the boundary layer is shown in figure 6 along with the experimental data. The variation of the skin friction coefficient with x and the growth of the boundary layer thickness are predicted very well. The velocity profiles at $x = 1.87\,m$ and $x = 2.55\,m$ are shown in figure 7. The agreement with the experimental data is again found to be reasonable.

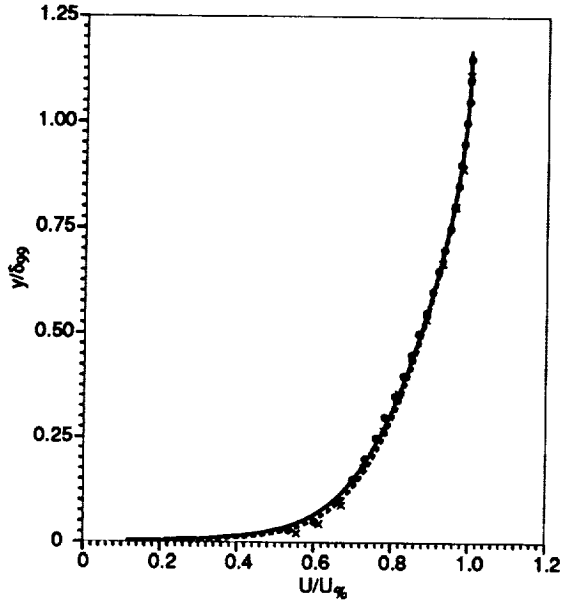

FIGURE 2. Similarity form of mean velocity profiles in zero pressure gradient boundary layer. •(——), $Re_\theta = 3195$; ×(- - -), $Re_\theta = 5473$.

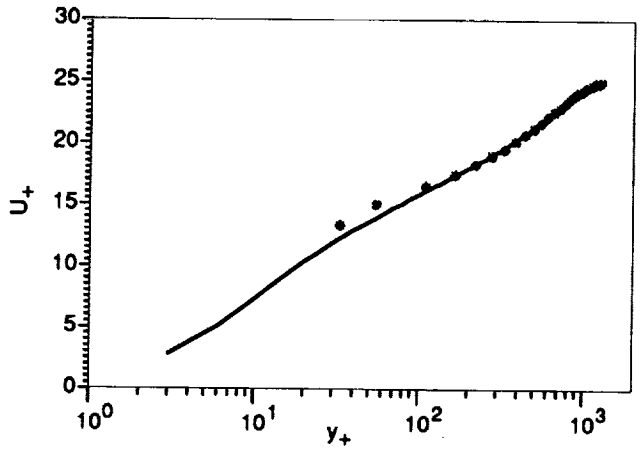

FIGURE 3. Log-linear plot of mean velocity profile in zero pressure gradient boundary layer.

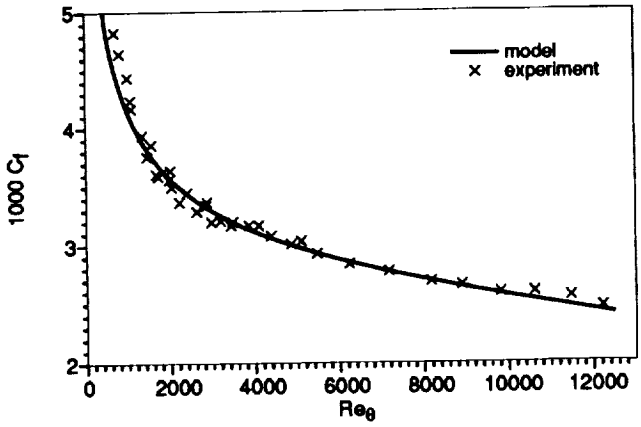

FIGURE 4. Skin friction coefficient versus momentum thickness Reynolds number for zero pressure gradient boundary layer.

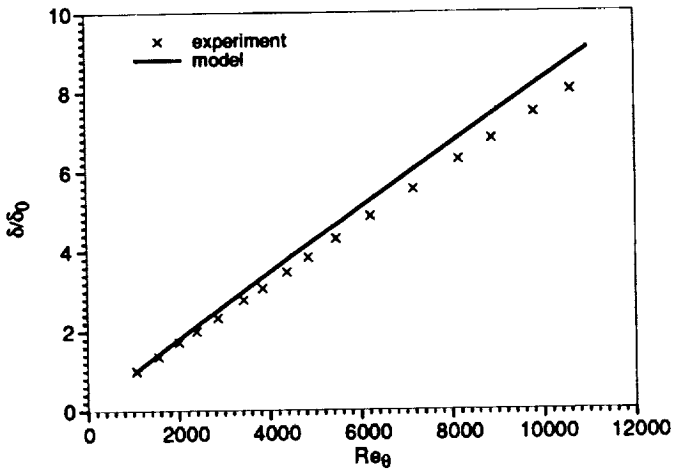

FIGURE 5. Boundary layer thickness versus Reynolds number for zero pressure gradient boundary layer.

4. Conclusions

We have presented a transport equation for eddy viscosity for wall bounded flows. Away from the wall, the proposed model reduces to a quasi-homogeneous model. The near wall effect is represented by an elliptic relaxation equation. Since geometrical information comes through the location where the boundary conditions are enforced while the model itself is free from the boundary information, the proposed

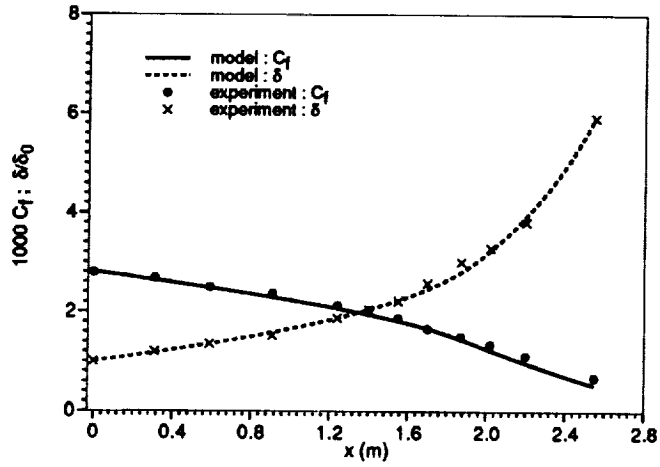

FIGURE 6. Skin friction coefficient and displacement thickness in the Samuel and Joubert boundary layer.

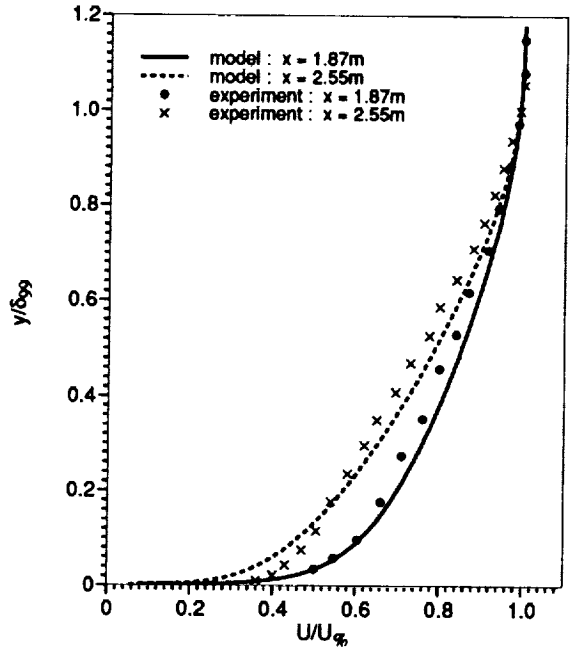

FIGURE 7. Mean velocity profiles at $x = 1.87\,m$ and $2.55\,m$ in the Samuel and Joubert boundary layer.

model has the potential to handle flows in complex geometry. All the quantities used in the model are local properties and are coordinate independent; the model is also Galilean invariant.

Channel flow at two Reynolds numbers and flat plate turbulent boundary layers with zero and adverse pressure gradients were calculated using the present model. The comparison with the DNS and experimental data were found to be quite promising.

Acknowledgement

Z. Y. would like to express his sincere thanks to Dr. T. Lund of CTR for his help during the Summer Program.

REFERENCES

BALDWIN, B. S. & BARTH, T. J. 1990 A one-equation turbulence transport model for high Reynolds number wall-bounded flows. *NASA TM* 102847.

BALDWIN, B. S. & LOMAX, H. 1978 Thin layer approximation and algebraic model for separated turbulent flows. *AIAA-78-256.*

CEBECI, T. & SMITH, A. M. O. 1974 *Analysis of turbulent boundary layers.* Academic Press.

COLES, D. E. & HIRST, E. A., eds. 1968 *Computation of turbulent boundary layers*, AFOSR-IFP-Stanford conference.

DURBIN, P. A. 1991 Near-wall turbulence closure modeling without 'damping functions'. *Theoret. Comp. Fluid Dynamics.* **3,** 1-13.

LAUNDER, B. E. & SPALDING, D. B. 1974 The Numerical Computation of Turbulent Flow. *Computer Methods in Applied Mechanics and Engineering.* **3,** 269-289.

NEE, V. W. & KOVASZNAY, L. S. G. 1968 The calculation of incompressible turbulent boundary layers by a simple theory. *Computation of turbulent boundary layers,* AFOSR-IFP-Stanford conference. 300-319.

RODI, W. 1980 *Turbulence Models and Their Application in Hydraulics.* Book Pub. of International Association for Hydraulic Research, Delft, the Netherlands.

SAMUEL, A. E. & JOUBERT, P. N. 1974 A boundary layer developing in an increasingly adverse pressure gradient. *J. Fluid Mech.* **66,** 481-505.

SPALART, P. R. & ALLMARAS, S. R. 1992 A one-equation turbulence model for aerodynamic flows. *AIAA-92-0439.*

IV. The combustion group

The combustion group conducted six projects. Three projects were related to premixed and three to non-premixed combustion. The invited participants were: Mr. M. Baum (Ecole Centrale Paris), Dr. J. H. Chen (Sandia National Laboratories); Prof. R. O. Fox (Kansas State University), Dr. D. C. Haworth (General Motors Research Laboratories), Prof. J. C. Hill (Iowa State University), Prof. S. Mahalingam (University of Colorado), Dr. T. Poinsot (Institut de Mécanique des Fluides de Toulouse), Prof. I. K. Puri (University of Illinois). The local participants were: Dr. R. D. Moser and Dr. M. M. Rogers from NASA Ames Research Center, and Dr. F. Gao, Dr. A. Trouvé, and Dr. L. Vervisch from the Center for Turbulence Research.

The broad scientific objectives of this group were similar to those of the CTR 1990 Summer Program: understanding of fundamental phenomena controlling turbulent combustion and application to modeling. However, the tools used in 1992 have covered a wider range: 2D or 3D, variable or constant density, simple or complex chemistry formulations for Direct Numerical Simulation (DNS) of turbulent combustion have been used. Recent progress in numerical analysis and code development have allowed us to use tools which were well adapted to the physical problems considered by each group.

The first three projects were aimed at increasing our understanding of turbulent premixed flames.

Poinsot & Haworth studied the interaction between a turbulent flame and a cold wall. Flame quenching distances as well as wall heat fluxes were measured from 2D simulations. The characteristics of flamelets reaching the wall (curvature, flame speed, quenching times) were used to build a 'law-of-the-wall' model for turbulent combustion. A simplified version of this model was derived and may be implemented in any flamelet model for turbulent premixed combustion.

A new 3D variable-density code was used by Trouvé & Poinsot to investigate the modeling of the evolution equation for the flame surface density. This analysis shows the limits of present flamelet models and suggests how the exact evolution equation for reactive surfaces may be closed to provide a suitable model. The effect of the Lewis number was evidenced and its influence on source or consumption terms for the flame surface density was demonstrated.

The first objective of the work by Baum, *et al.* was to prove the feasibility of DNS with complex chemistry and the potential of this approach for pollution studies. A second goal was to check whether the DNS results previously obtained with single-step chemistry are modified by accounting for more realistic chemical schemes. The project was based on a new 2D code where a DNS technique was coupled to CHEMKIN and TRANSPORT, the SANDIA packages for reacting flows with complex chemistry. Using this tool, it was possible to investigate the structure

of H2-O2 turbulent flames with the Warnatz scheme (9 species - 19 reactions). This project also provides the first analysis of the effects of stretch and curvature on flames with realistic chemistry.

The first project of Chen *et al.* was related to the effects of finite rate chemistry and differential diffusion on the structure of turbulent non-premixed flames. 3D variable-density simulations were performed over a range of conditions corresponding to fast and slow chemistry. This project provided new insights on the validity of the flamelet assumption as well as on the effects of transient regimes and small scales on the inner structure of the flame zone.

Chen *et al.* investigated one of the classical assumptions used to model turbulent non-premixed flames, *i.e.* single-step chemistry. Single-step and two-step chemical schemes were compared using 2D variable-density simulations of a non-premixed flame in isotropic turbulent flow. An important result was that extinction limits appear to be quite different: while single-step chemistry lead to multiple local extinctions, two-step chemistry feature more robust flames which do not quench.

DNS of a single-step chemical reaction with non-premixed reactants in forced isotropic turbulence were used by Fox *et al.* to obtain joint pdf's and other statistical information to parameterize and test a Fokker-Planck turbulent mixing model. The simulations were performed using a constant density, 3D spectral code developed by Moser and Rogers. Physical features as well as various statistics of the reacting scalars and their gradients were examined and compared to the model.

This Summer Program has brought many new and original results. The activity on non-premixed combustion was more intense than during previous programs and opened new perspectives for modeling for those flames. The demonstration that DNS of reacting flows was possible while taking into account complex chemistry or the presence of walls also opens new fields of investigations.

Modeling was one of our first objectives in this work. A fundamental aspect of the 1992 work is the impact and the power of DNS to answer certain critical questions for turbulent combustion models. We believe that DNS of reacting flows is now reaching a point where individual terms in combustion models may be estimated from DNS (as done by Trouvé & Poinsot) and that this possibility will change the way we construct models in the next few years.

Thierry J. Poinsot